

# Reduction in switching current using a low-saturation magnetization Co-Fe-(Cr, V)-B free layer in MgO-based magnetic tunnel junctions

著者	安藤 康夫
journal or publication title	Journal of Applied Physics
volume	105
number	7
page range	07D117-1-07D117-3
year	2009
URL	<a href="http://hdl.handle.net/10097/46554">http://hdl.handle.net/10097/46554</a>

doi: 10.1063/1.3068484

# Reduction in switching current using a low-saturation magnetization Co–Fe–(Cr, V)–B free layer in MgO-based magnetic tunnel junctions

Hitoshi Kubota,<sup>1,a)</sup> Akio Fukushima,<sup>1</sup> Kay Yakushiji,<sup>1</sup> Satoshi Yakata,<sup>1</sup> Shinji Yuasa,<sup>1</sup> Koji Ando,<sup>1</sup> Mikihiro Ogane,<sup>2</sup> Yasuo Ando,<sup>2</sup> and Terunobu Miyazaki<sup>3</sup>

<sup>1</sup>National Institute of Advanced Industrial Science and Technology (AIST), Central 2, Umezono 1-1-1, Tsukuba 305-8568, Japan

<sup>2</sup>Department of Applied Physics, Graduate School of Engineering, Tohoku University, Aoba-yama 6-6-05, Aramaki, Aoba-ku, Sendai 980-8579, Japan

<sup>3</sup>WPI Advanced Institute for Materials Research, Tohoku University, Katahira 2-1-1, Aoba-ku, Sendai 980-8577, Japan

(Presented 11 November 2008; received 17 September 2008; accepted 6 November 2008; published online 20 February 2009)

Magnetic properties, magnetoresistance (MR), and spin-transfer switching of magnetic tunnel junctions having a structure of Co<sub>60</sub>Fe<sub>20</sub>B<sub>20</sub> 3 nm/MgO 1 nm/(Co<sub>75</sub>Fe<sub>25</sub>)<sub>80-x</sub>Cr(V)<sub>x</sub>B<sub>20</sub> 2 nm ( $X=0-25$ ) were investigated. Magnetization of the (Co–Fe)–(Cr, V)–B free layer decreased from 1.2 T before substitution to 0.6 T at Cr of 10% (0.8 T at V of 10%). The MR ratio and a resistance-area product ( $RA$ ) before substitution were, respectively, about 130% and about  $2 \Omega \mu\text{m}^2$ . The MR ratio decreased to 80% at Cr of 10% and 40% at V of 10%. The  $RA$  values were almost independent of the composition. The intrinsic switching current density ( $J_{c0}$ ) decreased from 15 to 8 MA/cm<sup>2</sup> at Cr of 10% and 12 MA/cm<sup>2</sup> for V of 10%. Upon the further increase in Cr and V, stable switching was difficult to observe. In summary,  $J_{c0}$  decreased to half in the case of Cr, but the effect was small for V. © 2009 American Institute of Physics. [DOI: 10.1063/1.3068484]

## I. INTRODUCTION

The spin-transfer switching current for in-plane magnetized magnetic tunnel junctions (MTJs) is proportional to the product of the damping constant  $\alpha$  and the square of magnetization  $M_s$  of a free layer based on Slonczewski's model.<sup>1,2</sup> Lowering  $M_s$  is very effective in decreasing the switching current density ( $J_c$ ) for memory device applications.<sup>3</sup> Reportedly, CoFeB on MgO is amorphous in the as-deposited state and crystallizes into a bcc (100) oriented structure after annealing,<sup>4,5</sup> which is necessary for highly spin-polarized tunneling.<sup>6-8</sup> To decrease  $M_s$  of the free layer, we substitute Cr and V for Co–Fe because Cr metal and V metal exhibit a bcc structure, which would not affect the crystal structure of the free layer after annealing. For this study, we prepared MTJs with (Co–Fe)–(Cr or V)–B free layers and investigated their magnetic properties, magnetoresistance (MR), and spin-transfer switching as functions of the Cr and V concentrations.

## II. EXPERIMENTAL PROCEDURE

Using an UHV magnetron sputtering machine, substrate/buffer/Pt–Mn 15 nm/Co–Fe 2.5 nm/Ru 0.85 nm/Co<sub>60</sub>Fe<sub>20</sub>B<sub>20</sub> 3 nm/MgO 1 nm/(Co<sub>75</sub>Fe<sub>25</sub>)<sub>80-x</sub>Cr(V)<sub>x</sub>B<sub>20</sub> 2 nm ( $X=0-25$ )/cap thin films were prepared. The films were microstructured into  $70 \times 140 \text{ nm}^2$  elliptical shape using electron beam lithography combined with Ar ion etching. After microfabrication, the MTJs were annealed at 330 °C for 1 h under a 1 T magnetic field. Magnetization curves of

the plain films were measured at room temperature using a vibrating sample magnetometer. The magnetic field was swept between  $\pm 500$  Oe and the minor hysteresis loop due to free layer magnetization reversal was observed. MR curves were measured with a sense current of 1  $\mu\text{A}$  ac using a lock-in amplifier. The MR ratio is defined as  $(R_{\text{AP}} - R_{\text{P}})/R_{\text{P}} \times 100(\%)$ , where  $R_{\text{AP}}$  ( $R_{\text{P}}$ ) is the tunnel resistance when the magnetizations of the free layer and the bottom CoFeB layers are aligned antiparallel (AP) [parallel (P)]. Spin-transfer switching was observed by application of a sequential pulse current. The pulse width was 100 ms constant and the pulse height was varied between +2 and –2 mA with a step of 0.02 mA. The pulse sequence was repeated 100 times. From the distribution of switching current, intrinsic switching current ( $I_{c0}$ ) and thermal stability factor ( $\Delta$ ) were evaluated based on the thermally activated model.<sup>9-11</sup>

## III. RESULTS AND DISCUSSION

Figures 1(a)–1(d) depict the minor hysteresis loop of magnetization of the CoFeCrB free layers. The loop shifts in the  $+H$  direction are attributable to Néel coupling through the rough interface. The loop shifts in the  $+M$  direction<sup>10</sup> are attributable to the remanent magnetization of the Pt–Mn/Co–Fe/Ru/CoFeB bottom electrodes. Sharp magnetization reversals at low fields were observed for Cr concentrations of 0%–10%. The reversal became oblique at Cr of 15%, where coercivity was very small. For Cr of 20%, magnetization was very small and the distinct reversal disappeared. In the V case, magnetization curves showed similar variations with V concentration. Figure 1(e) portrays saturation magnetization ( $M_s$ ), which was obtained from the minor loops, as a func-

<sup>a)</sup>Electronic mail: hit-kubota@aist.go.jp.

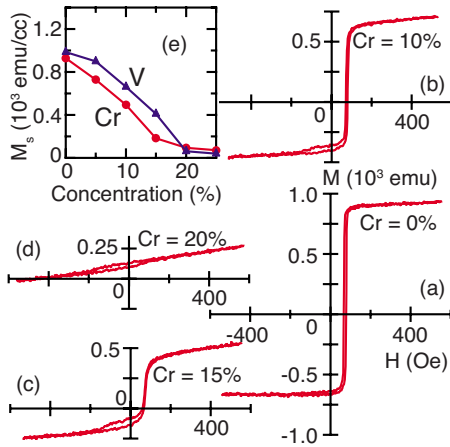


FIG. 1. (Color online) Minor hysteresis loops of the 2-nm-thick  $(\text{Co}_{75}\text{Fe}_{25})_{80-x}\text{Cr}_x\text{B}_{20}$  free layers with  $X=(a)$  0, (b) 10, (c) 15, and (d) 20. (e) Dependence of the magnetization on the concentrations of Cr and V.

tion of the Cr and V concentrations. The value of  $M_s$  decreased rapidly from 1.2 to 0.6 T for Cr of 10% and to 0.8 T for V of 10%. Further increased Cr and V concentrations reduced  $M_s$ , which was close to zero at around 20%.

Figures 2(a)–2(d) portray MR curves of the MTJs with Cr concentrations of 0%–15%. Sharp resistance jumps were observed in the MTJs with Cr of 0%–10%. However, at Cr of 15%, the curve showed two steps and indistinct hysteresis. Figure 2(e) shows the MR ratio as a function of Cr and V concentrations. At Cr of 0%, the MR ratio was about 130%. The MR ratio decreased rapidly to 80% at Cr of 10% and decreased linearly at higher Cr concentrations. In the V case, MR loops displayed a similar variation with increasing V concentration, but the MR ratio diminished faster. The resistance-area product ( $RA$ ) value was about  $2 \Omega \mu\text{m}^2$ , which was almost independent of Cr and V concentrations.

Figures 3(a) and 3(b) respectively present resistance-current ( $R$ - $I$ ) loops of the MTJs with Cr of 0% and 10%. Both samples showed a clear resistance jump because of spin-transfer induced magnetization reversals. In the loops, switching currents have distributions around mean values. The intrinsic switching current ( $I_{c0}$ ) was evaluated from the

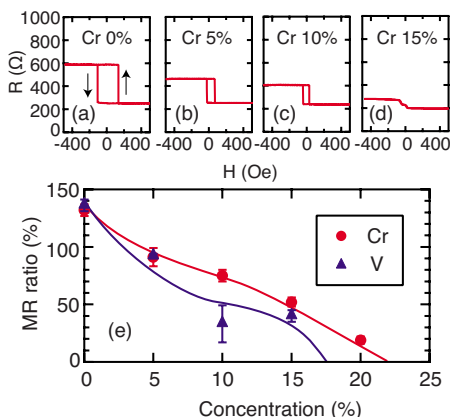


FIG. 2. (Color online) MR curves of the MTJs with  $(\text{Co}_{75}\text{Fe}_{25})_{80-x}\text{Cr}_x\text{B}_{20}$  free layers. The Cr concentrations are (a) 0, (b) 10, and (c) 15. (e) Dependence of the MR ratio on the concentrations of Cr and V. The lines are guide for the eyes.

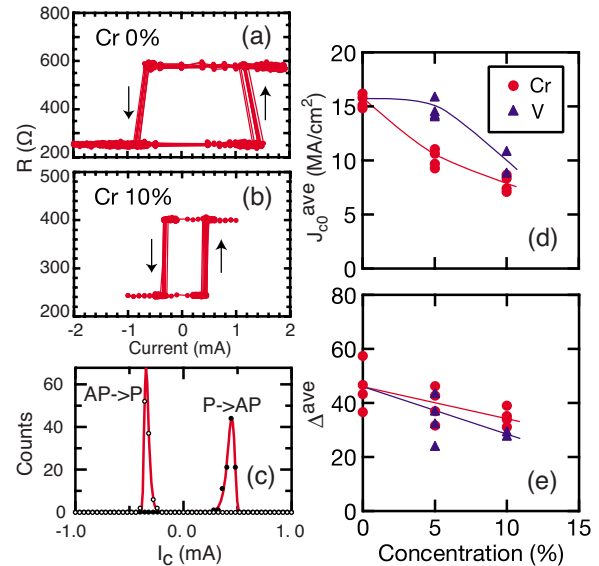


FIG. 3. (Color online) Resistance ( $R$ )-current ( $I$ ) loops of MTJs with (a)  $\text{Co}_{60}\text{Fe}_{20}\text{eB}_{20}$  and (b)  $\text{Co}_{53}\text{Fe}_{17}\text{Cr}_{10}\text{B}_{20}$  free layers. (c) Switching current ( $I_c$ ) distributions of the sample corresponding to (b).  $I_c > 0$  corresponds to switching from P to AP and  $I_c < 0$  to AP to P. The lines represent the theoretical fit based on Eq. (1) in the text. Concentration dependence of (d) averaged intrinsic switching current density ( $J_{c0}^{\text{ave}}$ ) and (e) averaged thermal stability ( $\Delta^{\text{ave}}$ ). The lines in (d) and (e) are guide for the eyes.

distribution of the observed switching current ( $I_c$ ) at a constant pulse duration (100 ms) based on a thermally activated spin-transfer switching model.<sup>9,10</sup> In the model, the distributions of  $I_c$  are expressed as

$$\frac{dP}{dI_c} = \Delta \frac{1}{I_{c0}} \frac{t_p}{\tau} \exp\left(-\frac{t_p}{\tau}\right), \quad (1)$$

where  $P$  signifies the switching probability,  $\Delta$  is the thermal stability,  $I_{c0}$  is the intrinsic switching current,  $t_p$  denotes the pulse duration, and  $\tau$  is the relaxation time, which is given as  $\tau = \tau_0 \exp\{\Delta[1 - I_c(t_p)/I_{c0}]\}$ . Actually,  $\tau_0$  is the inverse of attempt frequency, which is empirically inferred as 1 GHz. As depicted in Fig. 3(c), the experimental results were well explained by Eq. (1), where  $I_{c0}$  and  $\Delta$  are fitting parameters.<sup>10,11</sup> We analyzed both switching, AP to P and P to AP, and obtained two sets of  $I_{c0}$  and  $\Delta$  for one sample. The averaged intrinsic switching current density ( $J_{c0}^{\text{ave}} = (1/2) \times [I_{c0}(\text{P} \rightarrow \text{AP}) + I_{c0}(\text{AP} \rightarrow \text{P})]$ /junction area) and averaged thermal stability  $\Delta^{\text{ave}} = \{\Delta[(\text{P} \rightarrow \text{AP}) + \Delta(\text{AP} \rightarrow \text{P})/2]\}$  are portrayed, respectively, as functions of the concentrations of Cr and V in Figs. 3(d) and 3(e). In fact,  $J_{c0}^{\text{ave}}$  decreased from 15 to about 8 MA/cm<sup>2</sup> at Cr of 10% and to about 12 MA/cm<sup>2</sup> at V of 10%;  $\Delta^{\text{ave}}$  also decreased with increasing Cr and V concentrations from around 40 to 30. Upon further increase in Cr and V concentrations, switching in  $R$ - $I$  loops became very unstable. For that reason, reliable values were not obtained.

Theoretically,  $J_{c0}$  is expected to decrease proportionally to  $\alpha M_s^2$ .<sup>1,2</sup> Considering the reduced  $M_s$  by substituting Cr or V for Co-Fe,  $J_{c0}$  can be as small as one-fourth of the initial value at Cr of 10% and half of that at V of 10% if  $\alpha$  is constant. However, experimentally,  $J_{c0}$  was reduced to only half of the initial value at Cr of 10% and two-thirds at V of

10%. Therefore, the reduction in  $J_{c0}$  is less than that expected from the reduction in  $M_s$ . This reduction would result from increased  $\alpha$ , but that inference should be confirmed in future experiments. At compositions with Cr and V concentrations higher than 10%,  $J_{c0}$  was not evaluated because of its low thermal stability. In the present system, the energy potential between P and AP states is derived from the shape anisotropy of the elongated MTJ cell. The decreased  $M_s$  with increasing Cr and V concentrations, as presented in Fig. 2(e), corresponds to lowering the energy potential, resulting in the reduction in  $\Delta$ . If  $\Delta$  can be enhanced, for example, using magnetic coupling in a layered system,<sup>12</sup> even smaller  $J_{c0}$  is obtainable in compositions with Cr and V concentrations higher than 10%. The  $RA$  values were almost constant. Therefore, the influence of Cr and V on MgO tunnel barriers seems weak. The reduced MR ratios after the substitution suggest that Cr and V affected the electronic structure of CoFeB strongly. High-density memory devices require a larger MR ratio and a lower switching current density, for which effects of the substitution with Cr, V, and other elements on the band structure of CoFeB should be investigated.

## ACKNOWLEDGMENTS

This work was partially supported by the New Energy and Industrial Technology Development Organization (NEDO).

- <sup>1</sup>J. C. Slonczewski, *J. Magn. Magn. Mater.* **159**, L1 (1996).
- <sup>2</sup>E. B. Myers, D. C. Ralph, J. A. Katine, R. N. Louie, and R. A. Buhrman, *Science* **285**, 867 (1999).
- <sup>3</sup>K. Yagami, A. A. Tulapurkar, A. Fukushima, and Y. Suzuki, *Appl. Phys. Lett.* **85**, 5634 (2004).
- <sup>4</sup>D. D. Djayaprawira, K. Tsunekawa, M. Nagai, H. Maehara, S. Yamagata, and N. Watanabe, *Appl. Phys. Lett.* **86**, 092502 (2005).
- <sup>5</sup>S. Yuasa, Y. Suzuki, T. Katayama, and K. Ando, *Appl. Phys. Lett.* **87**, 242503 (2005).
- <sup>6</sup>W. H. Butler, X.-G. Zhang, T. C. Schulthess, and J. M. MacLaren, *Phys. Rev. B* **63**, 054416 (2001).
- <sup>7</sup>S. Yuasa, T. Nagahama, A. Fukushima, Y. Suzuki, and K. Ando, *Nature Mater.* **3**, 868 (2004).
- <sup>8</sup>S. S. P. Parkin, C. Kaiser, A. Panchula, P. M. Rice, B. Hughes, M. Samant, and S. H. Yang, *Nature Mater.* **3**, 862 (2004).
- <sup>9</sup>R. H. Koch, J. A. Katine, and J. Z. Sun, *Phys. Rev. Lett.* **92**, 088302 (2004).
- <sup>10</sup>M. Pakala, Y. M. Huai, T. Valet, Y. F. Ding, and Z. T. Diao, *J. Appl. Phys.* **98**, 056107 (2005).
- <sup>11</sup>M. Morota, A. Fukushima, H. Kubota, K. Yakushiji, S. Yuasa, and K. Ando, *J. Appl. Phys.* **103**, 07A707 (2008).
- <sup>12</sup>J. Hayakawa, S. Ikeda, Y. M. Lee, R. Sasaki, T. Meguro, F. Matsukura, H. Takahashi, and H. Ohno, *Jpn. J. Appl. Phys., Part 2* **45**, L1057 (2006).